Experimental Model and Immunohistochemical Analyses of U87 Human Glioblastoma Cell Xenografts in Immunosuppressed Rat Brains

TADEJ STROJNIK[1], RAJKO KAVALAR[2] and TAMARA T. LAH[3]

[1]Department of Neurosurgery and [2]Department of Pathology, Maribor Teaching Hospital, Ljubljanska 5, SI-2000 Maribor; [3]Department of Genetic Toxicology and Cancer Biology, National Institute of Biology, Vecna pot 111, SI-1000 Ljubljana, Slovenia

Abstract. *Background: To study the neuropathology and selected tumour markers of malignant gliomas, an animal glioma model was developed using the implantation of human glioblastoma clone U87 into rat brains. Materials and Methods: The U87 cell suspension, or precultured U87 tumour spheroids, were inoculated into the brain of 4-week-old cyclosporin A immunosuppressed Wistar rats. The resulting first generation tumours were then transferred, through serial transplantations to rats, to obtain second and third generation tumours. Brain tumour sections were examined for various known tumour markers by routine HE staining and immunohistochemical analyses. Results: The immunohistochemical analyses showed that p53, S100 protein, glial fibrillary acidic protein (GFAP) and synaptophysin expressions, initially present in the tissue culture, were gradually lost in later tumour generations, whereas nestin and musashi expressions increased, possibly indicating progressive tumour cell dedifferentation. Persistent kallikrein, CD68 and vimentin expressions in U87 cells, as well as in all the generations of tumours, may be related to the preservation of the mesenchymal cell phenotype in this tumorigenesis model. Decreased cathepsins expression indicated lower invasive potential, but increasing Ki-67 expression marked higher proliferation activity in the subsequent tumour generations. The strong immune reaction for FVIII in the second and third generation tumours correlated with the observed increase in vascular proliferation in these tumours. Conclusion: A simple, and well-defined rat model of fast-growing glioma was established, providing a basis for further experimental studies of genetic and protein expression fingerprints during human glioma tumorigenesis.*

Correspondence to: Tadej Strojnik, Department of Neurosurgery, Maribor Teaching Hospital, Ljubljanska 5, SI-2000 Maribor, Slovenia. Tel: +386 2 321 1511, Fax: +386 2 332 4830, e-mail: t.strojnik@siol.net

Key Words: Angiogenesis, dedifferentiation, experimental cancer rat model, glioma, invasion, tumour markers, U87 spheroids.

The objective of experimental neuro-oncology is to contribute to a better understanding of human malignant brain tumours (1). To this end, the development of several animal models has provided specific clues about the formation of gliomas (2). Such animal models are also beneficial for selective molecular and biochemical analyses of tumour markers (3). Heterotransplant models hold great potential for studying the expression of markers which translate into the phenotypic behaviour of consecutive tumour generations. It has been proposed that, with serial passages, highly malignant cell populations are selected, which cause a decrease in the latent period and an increase in the tumour growth rate (4). The culture of human glial tumours has long been recognized, not only as a tool for gaining additional diagnostic (prognostic) information and to planning individualized therapies, but also for a better understanding of brain tumour cell biology. Glial tumours are made up of heterogeneous cell populations. Vascular elements (endothelial cells, pericytes) and other mesenchyme-derived cells (fibroblasts, microglia) in the tumour also contribute to its behaviour (4).

Multicellular tumour spheroids from human gliomas have been introduced as a model for the study of brain tumour invasion (5-7). Since all these cell types can grow *in vitro*, the cultures must be characterized to ascertain the cell subpopulations which have been selected through the culture conditions. Morphological characterization is not sufficient and a panel of markers may be required to define the populations present. However, as the cells adapt to the tissue culture conditions, they may lose the ability to express one or more of these markers. The need for better and more relevant brain tumour models is generally acknowledged.

In the present study, a tumorigenesis model was developed, originating from tumour spheroids prepared from the U87 human glioblastoma cell line, in the brain of

Wistar rats, which were immunosuppressed with cyclosporine A. U87 cells are considered to be a rapidly proliferating cell line, which can be grown in culture as monolayers and tumour spheroids (Figure 1a,b). Tumours that were induced by this procedure were also transferred through serial transplantations from rat to rat. Our technique was simple, reproducible and associated with a high tumour take rate in 2 to 3 weeks. This model, if similarities with *in vivo* human glioma progression are found, would offer the opportunity to compare the expression of various immunohistochemical markers of U87 cells and spheroids in culture in rat brain, in order to understand the biology of tumour progression and the possible interference at the molecular level of down-regulating the most relevant factors responsible for this progression.

Materials and Methods

U87 glioma clone and culture conditions. U87 is a highly malignant anaplastic glioma clone derived from a 44-year-old Caucasian woman. Its *in vitro* and *in vivo* growth characteristics have been described in detail (8-10). The cells were grown in plastic 75-cm^2 flasks with Vent Cap (Corning, Acton, MA, USA). The cell lines were routinely maintained in tissue culture medium, consisting of Dulbecco's modified Eagle's medium (DMEM) (Sigma, St. Louis, MO, USA) containing 10% heat-inactivated foetal bovine serum, 2% L-glutamine, penicillin (100 IU/ml) and streptomycin (100 μg/ml). The flasks were kept in a standard tissue culture incubator (100% relative humidity, 95% air and 5% CO_2) (Forma Scientific, USA) and studied daily by phase-contrast microscopy (Euromex, The Netherlands). The culture medium was changed twice weekly.

For transplantations and spheroid formation, the monolayer of cells in culture were trypsinized (Trypsin-EDTA Gibco, Invitrogen Corporation), washed in phosphate-buffered saline (PBS), pH 7.4, (Sigma-Aldrich Cheme, Steinheim, Germany) and suspended in tissue culture medium. The cell number was determined by counting the cells in a haemocytometer (Neubauer improved, Labor Optik) and the percentage of living cells was evaluated by Trypan blue (Sigma-Aldrich Cheme) exclusion.

Rat tumour tissue for tumour transplantation and for spheroid formation. Two weeks after inoculation, the rats were anaesthetized by intramuscular (*i.m.*) injection of 80-100 mg/kg 10% ketamin and 3-4 mg/kg 2% xylasin. Under sterile conditions, the inoculation site was exposed, additional bone was removed using a dental drill and the tumour was dissected under the operating microscope. The specimens were immediately aseptically transferred to a tissue culture dish (Orange Scientific, Braine-l'Alleud, Belgium) containing tissue culture medium. Specimens selected for spheroid formation and for rat implantation were cut with scalpels into 0.5- to 1-mm pieces. Representative samples were also fixed in 10% buffered formalin for histological and immunohistochemical (IHC) assessment.

Spheroid cell growth. For spheroid formation, the U87 cell suspension or 0.5-mm tumour fragments were put into a 60-mm Ultra Low Attachment Dish (Corning Inc., NY, USA). The Ultra Low Attachment surface is a covalently bound hydrogel layer that is hydrophilic and neutrally charged, preventing cell attachment. The surface was rehydrated with medium 15 min prior to the addition of the cells or tumour fragments. The rehydration medium was aspirated and 5 ml of fresh medium was added. The dishes were kept in a standard tissue culture incubator as described above. The spheroids were studied daily by phase-contrast microscope, and the medium was changed every week. Spheroids for inoculation into the brains of normal rats, ranging from 200 to 300 μm in diameter, were selected using a micropipette and a stereomicroscope with a calibrated reticle in the eyepiece. The spheroids were cultured for up to 30 days, at which time they were fixed for histology and immunohistochemistry.

Tumour-glioblastoma progression models in rats. All procedures and experiments involving animals in this study were approved by the Veterinary Administration of the Republic of Slovenia and conducted according to the European Convention for the Protection of Vertebrates Used for Scientific Purposes. The hosts were fifteen normal 4-week-old Wistar Hanover rats (120-150 g) (Medical Faculty, Institute of Pathology, Ljubljana, Slovenia). The animals were kept at 25˚C in a specific pathogen-free environment, on a standard 12-h night and day cycle. The U87 cell suspension and U87 cell spheroids (Sph-I generation, first generation spheroids) were injected into three animals and transplanted into the brain in seven animals, respectively, giving rise to the ten tumours of the first generation (Tumours-I generation). Out of these tumours, three were cut in pieces and the cell spheroids were grown under the same conditions as spheroids from the first generation, giving rise to the Sph-II generation. For the second implantation, the tumour pieces (of Tumour-I generation) were implanted into three rats and the tumours of the second generation (Tumour-II generation) were grown in the rats. After 2 weeks, two tumours were excised, cut into pieces and implanted again into rats, giving rise to tumours of the third generation (Tumour-III generation). From the tumours of the II generation spheroids were prepared (Sph-III generation) for analyses of biological markers. The spheroids were not further transplanted into the rats.

At the time of the experiments, the rats were anaesthetized by *i.m.* injection of 80-100 mg/kg 10% ketamin and 3-4 mg/kg 2% xylasin. The animals were mounted in a small-animal stereotactic frame (Stoelting, USA) and, after washing the skin of the head, a midline incision was made in the scalp to expose the skull. A small hole was drilled 1-2 mm to the right of the midline fissure and 1-2 mm posterior to the bregma of the animal's skull using a dental drill.

For intracranial inoculation of the single cell suspension and spheroids, a Hamilton (Hamilton, Bonaduz, Switzerland) syringe was used. The syringe was washed with 70% alcohol and flushed with sterile saline before, and with sterile water after, use. The syringe was placed in the syringe holder of the stereotactic frame. The needle was then placed 2.5 mm below the surface of the brain and the single cell suspension or spheroids were slowly injected into the brain, after which the needle was slowly withdrawn and the skin wound was closed. For the implantation of tumour pieces, a slightly larger hole was drilled, the dura was opened and tumour pieces were inoculated under the microscope into the subcortical white matter.

The inflammatory reaction against the human glioma cells was inhibited with cyclosporin A (50 mg/ml; Novartis, Basel, Switzerland), *i.m.* injections (12 mg/kg/d) daily.

The animals were sacrificed 1, 2 and 3 weeks post-implantation. For *in situ* perfusion of the brain, the animals were anaesthetized

as described. Thoracotomy was performed and the left ventricle was canulated. The descending aorta was clamped. After rinsing with 0.9% NaCl, the animals were perfused with 10% formalin in PBS (pH 7.4). Right atriotomy was performed immediately after starting to rinse. The brain was then left within the skull for 24 h at room temperature. After removal, it was placed into rodent brain matrices and cut in the coronal plane. Thereafter, transverse slides were embedded in paraffin. Five-micrometer sections were stained with haematoxylin and eosin (HE) and labelled for the presence of different markers.

Immunohistochemical analysis. IHC staining was performed using the standard technique, according to the protocol of the Department of Pathology at the Maribor Teaching Hospital, Slovenia. The U87 cell suspension was centrifuged at 2500 rpm for 15 min, the supernatant poured off and the cell sediment resuspended in 0.5% bovine serum albumin (BSA; Serva, Heidelberg, Germany). Smears were fixed in methanol for 1 h and then treated with methanol peroxide solution for 15 min. Pre-cultured spheroids were placed in 10% buffered formalin for fixation. Five-μm-thick sections, sliced from paraffin-embedded specimens, were mounted on glass slides precoated with silane and dried overnight at 37˚C, and then at 57˚C for 8 h. After deparaffinizing in xylene and washing in a graded series of ethanol, the sections were placed in a 10 mmol/l sodium citrate buffer (pH 6.0) and boiled for 12 min at 110˚C in a Microwave Vacuum Histoprocessor (Milestone RHS-1, Shelton, CT, USA) for antigen retrieval. The slides were incubated with the primary antibodies raised against the Ki-67 marker of the proliferation monoclonal antibody (MAb) (1:50 dilution; DAKO, Glostrup, Denmark), p53 tumour suppressor protein MAb (1:150 dilution; DAKO), vimentin developmentally-regulated intermediate filament MAb (1:300 dilution; DAKO), S100 protein, glial and ependymal cell marker polyclonal antibody (PAb) (1:2500 dilution; DAKO), GFAP astrocyte specific glial fibrillary acidic protein PAb (1:2500; DAKO), nestin stem cell marker anti-human PAb (1:1000 dilution; Karolinska Institute, Stockholm, Sweden), musashi stem cell marker anti-human PAb (1:1000 dilution; Chemicon Inc., CA, USA), synaptophysin marker of neuroendocrinal function PAb (1:50 dilution; DAKO), cathepsin B cystein protease MAb (1:100 dilution; clone 3E1, KRKA, d.d. Novo mesto, Slovenia), cathepsin L cysteine protease MAb (1:10 dilution; clone N135, KRKA), CD68 macrophage and microglia marker anti-human MAb (1:50 dilution; DAKO), FVIII endothelial cell marker Ab (1:2000 dilution; DAKO) and human kallikrein 6 serine protease PAb (1:400 dilution; Mount Sinai Hospital, Toronto, Canada).

All incubations were carried out overnight at 4˚C. After washing in Tris-buffered saline, immunoperoxidase staining was performed by an EnVision Ab complex method using the ENVISION kit (DAKO) (11). After rinsing in tap water, the sections were counterstained with Mayer's haematoxylin and mounted.

Nuclear staining of Ki-67 was considered positive. The Ki-67 staining index (SI) was defined as the percentage of positive nuclei of a total of 2,000 tumour cells counted using an eyepiece grid (12). p53 staining was considered positive if more than 10% of the tumour cells showed nuclear staining and negative if less than 10% of the tumour cells showed nuclear staining (13). Immunoreactivity for the other brain-associated cell markers listed above was evaluated as negative (0) when no positive immunoreaction in the cells was observed within the tumour, weak (+) when less than 30% of the tumour cells were positive, moderate (++) when 30-60% of the tumour cells were positive, and strong (+++) when more than 60% of the tumour cells were positive. Twenty representative fields were counted using x40 magnification.

Slides stained with omission of the primary antibody served as negative controls for Ki-67 and p53 staining. Positive controls for S100 protein, synaptophysin, GFAP, vimentin kallikrein, FVIII (vessels) and cathepsin L (pyramidal cells) were performed using normal brain sections. Liver tissue sections were used as a positive control for cathepsin B and spleen for the macrophage surface marker CD68. One glioblastoma specimen was used as a nestin- and musashi-positive control sample, while an adenocarcinoma brain metastasis was used as a nestin- and musashi-negative control (14).

Results

Clinical course. After intracerebral transplantation, the animals quickly recovered. One week later, four animals were sacrificed. The other eleven animals remained neurologically intact for 1 week. Thereafter, five out of the eleven animals exhibited symptoms of raised intracranial pressure with restlessness, convulsions and paresis on the opposite side from the operation, whereas the remaining six animals were without obvious neurological effects.

Macroscopic findings. Initial tumour growth was already seen 1 week after transplantation in three animals (spheroid Tumour-I gen., Tumour-II gen., Tumour-III gen.). The tumours were solid, spherical in shape and grey-red in colour. They measured approximately 2x2x2 mm and were surrounded with a zone of oedema. One week after inoculation of a $3x10^6$ cell suspension, a narrow, somewhat haemorrhagic, injection channel with small tumour nodules, approximately 1 mm in diameter, could only just be detected (Figure 2b). After 2 weeks, three animals with first generation tumours (all received spheroid injection) and two animals with second generation tumours were sacrificed. Spreading of the tumour through the hole into the subcutaneous tissue was noted in two out of three animals with U87 spheroid-induced first generation tumours and in both animals with second generation tumours. The tumours in those animals were lobulated in shape and had reached a size of approximately 3x2x2 mm (Figure 2a). In the remaining animal, the U87 spheroid-induced first generation tumour measured 4x2x2 mm, extending through the entire right hemisphere but remaining within the brain. After 3 weeks, the tumours had reached their maximum size, measuring approximately 5x3x3 mm in the remaining three animals of the U87 spheroid-induced first generation tumour and in one animal with third generation tumour. In all the animals, the tumour had spread through the hole in the subcutaneous tissue. Peritumorous oedema within the ipsilateral hemisphere and a shift of the midline to the opposite side

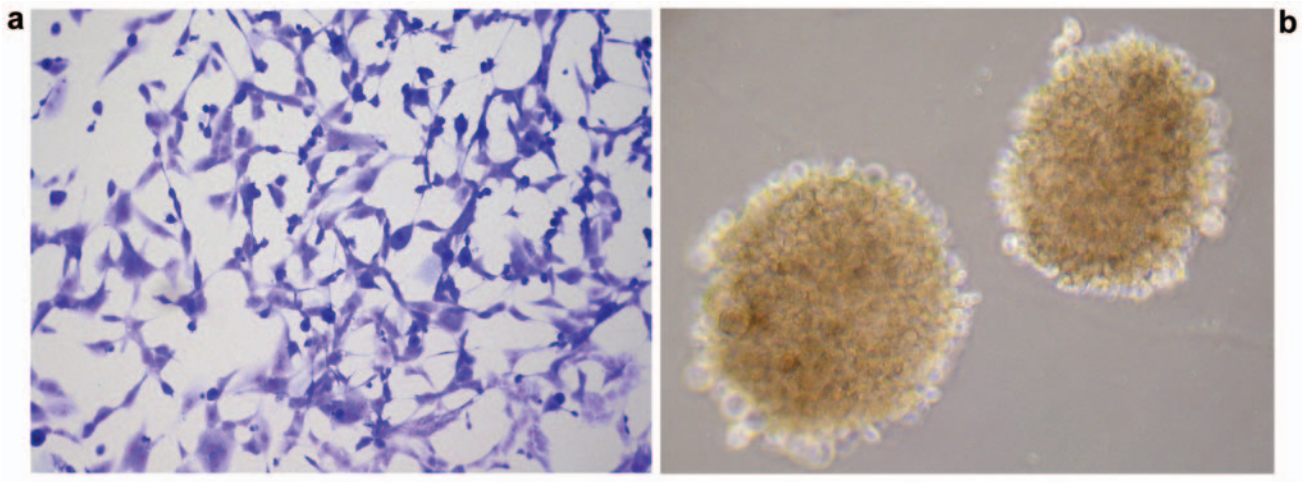

Figure 1. *Photographs of U87 human glioma cells grown in culture as a) monolayer (Pappenheim, x10) and b) spheroids (phase contrast, x10).*

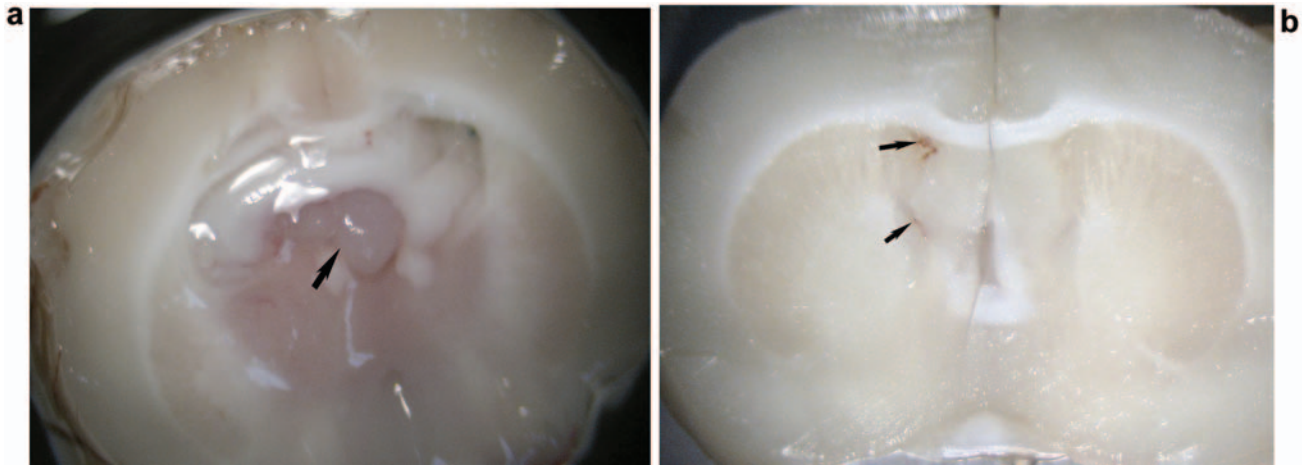

Figure 2. *a) Coronal brain tissue sections demonstrated solid, lobulated, greyish tumour in the region of the right basal ganglia 2 weeks after inoculation of U87 spheroids (arrow); b) One week after inoculation of a 3x10^6 cell suspension, a narrow, somewhat haemorrhagic, injection channel with small tumour nodules approximately 1 mm in diameter could just be detected (arrows).*

were most prominent after 3 weeks. In the remaining two animals, which had received the cell suspension, only small tumour nodules approximately 1.5 mm in diameter could be detected, and brain oedema was present, but not so extensively as in the previous group.

Histopathology

First generation tumours obtained from U87 cell suspension: One week after transplantation of 3x10^6 cells into the brain, coronal whole brain sections demonstrated a narrow haemorrhagic injection channel through the white matter to the basal ganglia. Tumour cells, an oedematous reaction of the surrounding brain, microcalcifications, siderophages and widespread leukocyte infiltration were observed (Figure 3A). After 3 weeks, small solid tumour nodules, of 0.5 to 1 mm in diameter, extended along the injection channel in both the remaining animals. The tumour growth was characterized by the formation of multiple and small tumour nodules infiltrating the neighbouring brain tissue more or less irregularly. The cells were spindle-shaped or polygonal and contained round or oval hypochromatic nuclei with nucleoli (Figure 3b). They had a tendency to grow closely packed in whorls and streams. Many mitoses demonstrated rapid growth. Regressive changes with cyst formation were observed in some of these tumours. The tumour nodules appeared to be connected by a narrow band of tumour cells running in the subarachnoid space (Figure 3c).

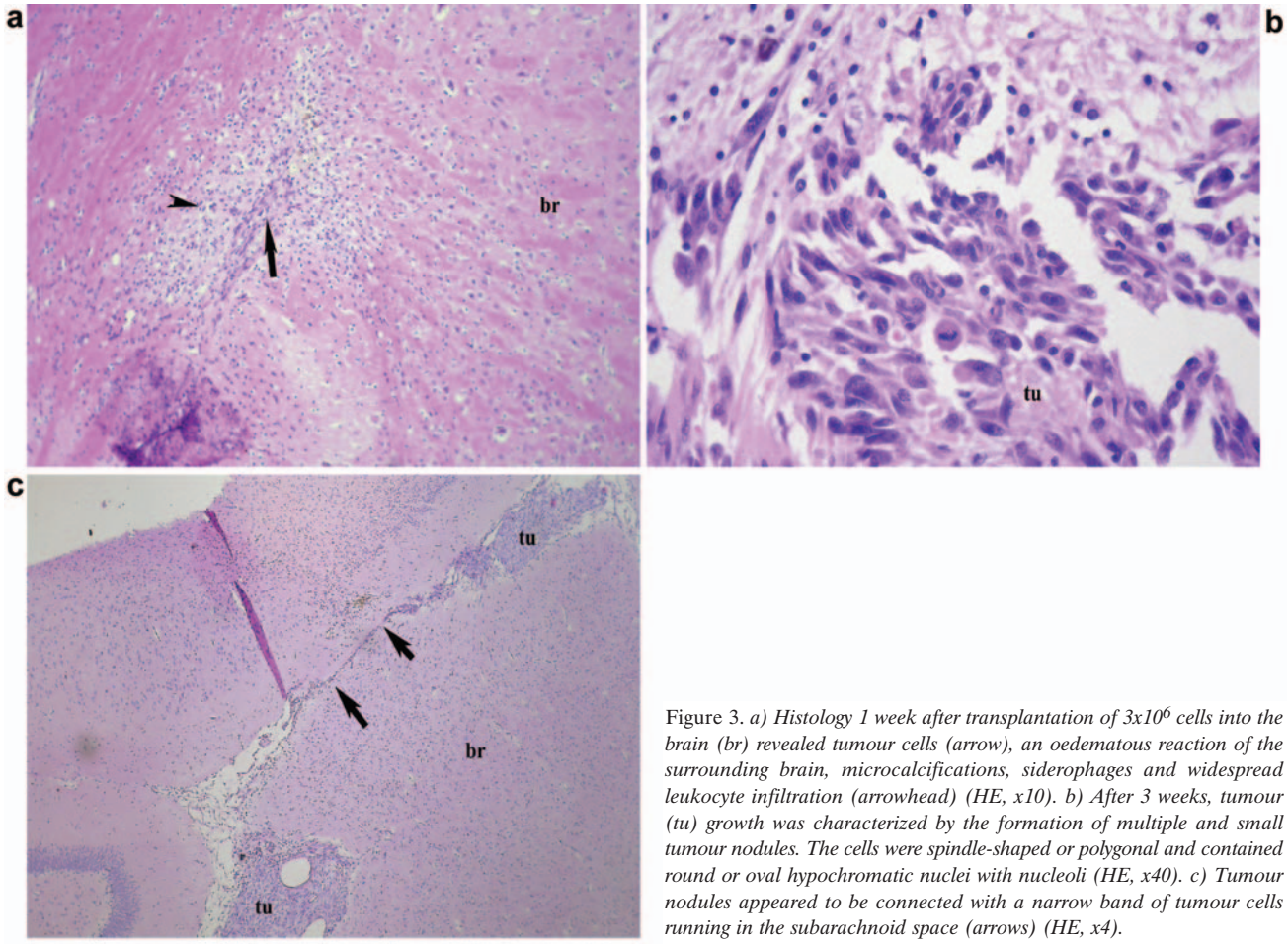

Figure 3. *a) Histology 1 week after transplantation of $3x10^6$ cells into the brain (br) revealed tumour cells (arrow), an oedematous reaction of the surrounding brain, microcalcifications, siderophages and widespread leukocyte infiltration (arrowhead) (HE, x10). b) After 3 weeks, tumour (tu) growth was characterized by the formation of multiple and small tumour nodules. The cells were spindle-shaped or polygonal and contained round or oval hypochromatic nuclei with nucleoli (HE, x40). c) Tumour nodules appeared to be connected with a narrow band of tumour cells running in the subarachnoid space (arrows) (HE, x4).*

First generation tumours obtained from U87 cell spheroids: After 1 week, an irregular 2 mm in diameter tumour was seen just underneath the corpus callosum. The tumour was sharply demarcated against the surrounding brain tissue, but invaded the choroid plexus and was spreading towards the ventricles (Figure 4a). A narrow band of leukocyte infiltrate, consisting of granulocytes and lymphocytes, surrounded the tumour (Figure 4b), while the surrounding brain was oedematous. Within the tumour, polygonal cells were densely packed and many mitoses demonstrated rapid growth (Figure 4c). After 2 weeks, the tumour size had increased and reached approximately 3 to 4 mm in diameter. The tumours were fairly large and irregular with extensive oedema reactions, especially in the white matter of the homolateral hemisphere. In the tumour periphery, numerous blood vessels demonstrated tumour neovascularization, whereas leukocyte infiltration was less expressed (Figure 4d). After 3 weeks, the tumours had reached their maximum size with a diameter of approximately 5 mm. Solid tumour areas were composed of densely-packed polygonal cells. The polymitotic tissue with numerous tumour cells indicated rapid growth. Inside the tumour, there were several small areas of tumour necrosis. In the neighbourhood of the tumours, especially in the white matter of the ipsilateral hemisphere, marked oedema had developed.

Second generation tumour: One week after implantation of the first generation tumour, the tumour had reached approximately 2 to 3 mm in diameter. The tumour border appeared irregular. The spongiform state of perifocal oedema was restricted to a narrow zone around the tumour. A broader band of leukocyte infiltrate, consisting of granulocytes and lymphocytes, surrounded the tumour, especially at its base. No necroses and only a few tumour blood vessels could be observed. Stream-like solid patterns contained fine reticulin fibres. Many mitoses indicated rapid growth. The cells were spindle-shaped or polygonal and contained oval hypochromatic nuclei with nucleoli. After 2 weeks, the tumours were clearly larger and surrounded with extensive brain oedema, which extended into the

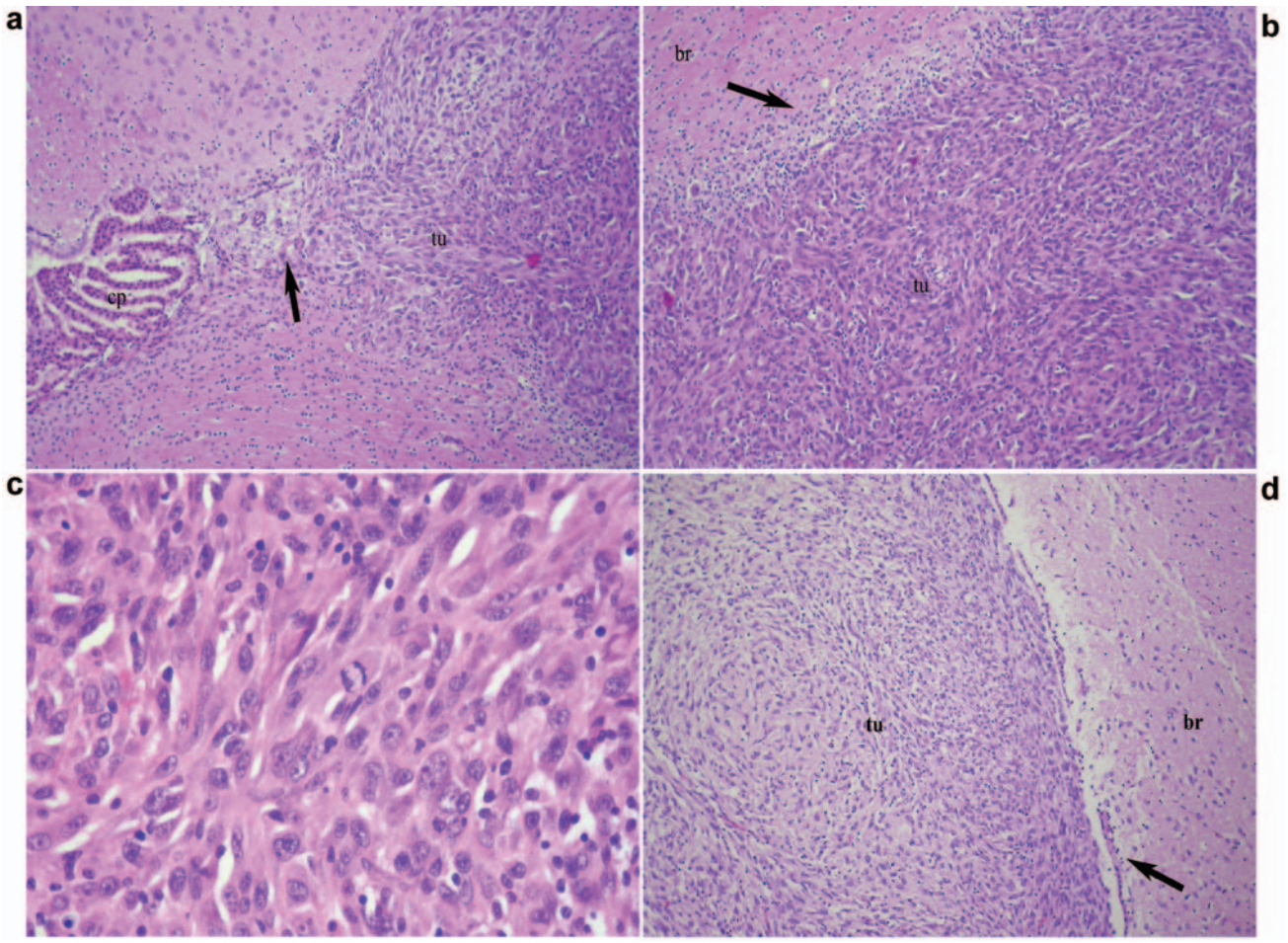

Figure 4. *a) One week after inoculation of spheroids, a tumour demarcated against the surrounding brain tissue, but invading the choroid plexus (cp) and spreading toward the ventricles, was seen (arrow) (HE, x10). b) A narrow band of leukocyte infiltrate, consisting of granulocytes and lymphocytes, surrounded the tumour (arrow) (HE, x10). c) Within the tumour, polygonal cells were densely packed and many mitoses demonstrated rapid growth (HE, x40). d) After 2 weeks, in the tumour periphery numerous blood vessels demonstrated tumour neovascularization, whereas leukocyte infiltration was less expressed (arrow) (HE, x10).*

surrounding white matter, whereas leukocyte infiltration was less expressed. Inside the tumour, small areas of coagulation necrosis and some vessels could be detected.

Third generation tumour: The tumour had reached approximately 3 to 4 mm in diameter as early as 1 week after implantation. A broad band of leukocyte infiltrate, consisting of granulocytes and lymphocytes, surrounded the tumour (Figure 5a). The tumour border appeared irregular. Inside the tumour, numerous tumour blood vessels and areas of coagulation necrosis were observed (Figure 5b). Many mitoses indicated rapid growth. After 3 weeks, a huge tumour, measuring nearly 6 mm in diameter and penetrating into the subcutaneous tissue, had developed. The tumour consisted of numerous tumour vessels, areas of coagulation necroses and a cell population which was heterogeneous, consisting not only of spindle-shaped or polygonal cells with oval hypochromatic nuclei with nucleoli, but also bizarre gigantic cells with hyperchromatic round nuclei (Figure 5c). Again, many mitoses indicated rapid tumour growth (Figure 5d).

Immunohistochemistry. Immunostaining was evaluated as described in Materials and Methods. The results of the immunostaining are summarized in Table I.

The index of proliferation, Ki-67 LI, increased from a mean value of 45% in the U87 cell suspension to 75-80% in the tumour (Figure 6a,b). In the spheroids, more nuclei were positive on the periphery. In the U87 cell suspension, more than 10% of the tumour cells showed p53 nuclear staining, whereas in the spheroids and in the tumour the staining was negative (Figure 6c). Most of the tumour cells presented a strong immune reaction for vimentin (Figure 6d). Reactive astrocytes, cells of the ependyma, choroid

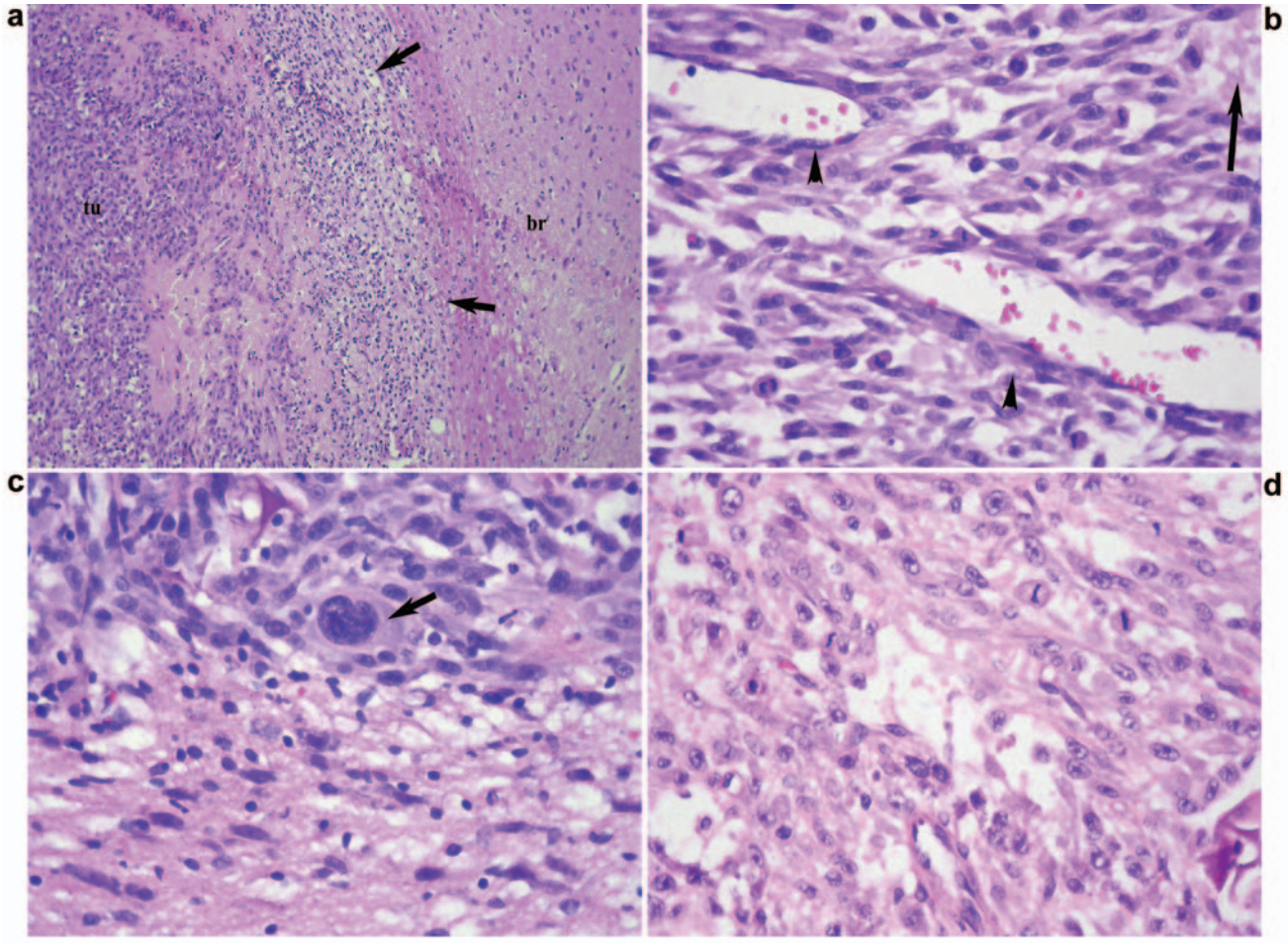

Figure 5. *a) Third generation tumour 1 week after implantation. A broad band of leukocyte infiltrate, consisting of granulocytes and lymphocytes, surrounded the tumour (arrow) (HE, x10). b) Inside the tumour, numerous tumour blood vessels (arrowhead) and areas of coagulation necrosis (arrow) could be observed (HE, x40). c) The tumour consisted of numerous tumour vessels, areas of coagulation necroses and a cell population which was heterogeneous, consisting not only of polygonal cells with oval hypochromatic nuclei, but also bizarre gigantic cells with hyperchromatic round nuclei (arrow) (HE, x40). d) Many mitoses indicated rapid tumour growth (HE, x40).*

plexus and vascular endothelia were vimentin-negative. The expression of the S100 protein was moderate in the cells in suspension and minimal in the tumour cells of the spheroids and tumour, whereas strong immunostaining was noted in the surrounding normal and oedematous brain tissue, especially reactive astrocytes (Figure 6e). The cell suspension expressed glial fibrillary acidic protein (GFAP) to a moderate degree, but the spheroids and the tumours were GFAP-negative. Normal and oedematous brain tissue showed an intense expression of GFAP in nearly all astroglial cells. Reactive astrocytes within the peritumorous oedema lesion revealed strong positive immunoreactivity (Figure 6f). Weak nestin staining was revealed in the cell suspension, but not in the spheroids. The expression of nestin increased in the tumour cells and vascular endothelia of the tumours to a moderate degree (Figure 6g,h). The expression of musashi was minimal in the cell suspension, whereas tumour cells in the spheorids and tumours presented a moderate immune reaction (Figure 7a). Tumour cells in the suspension expressed moderate synaptophysin immunoreactivity, whereas the tumour cell expression in the spheroids and tumours was minimal (Figure 7b). The surrounding brain tissue displayed an intense expression of synaptophysin. Most of the tumours cells in the cell suspension, first generation spheroids and first generation tumours presented strong immune reactions for cathepsin B, whereas the expression in the second and third generation spheroids and tumours was weak to moderate. Besides the tumour cells, staining in the vascular endothelia was noted (Figure 7c). Staining with the cathepsin L antibody revealed a strong positive reaction in the cells in suspension. The spheroids presented a moderate

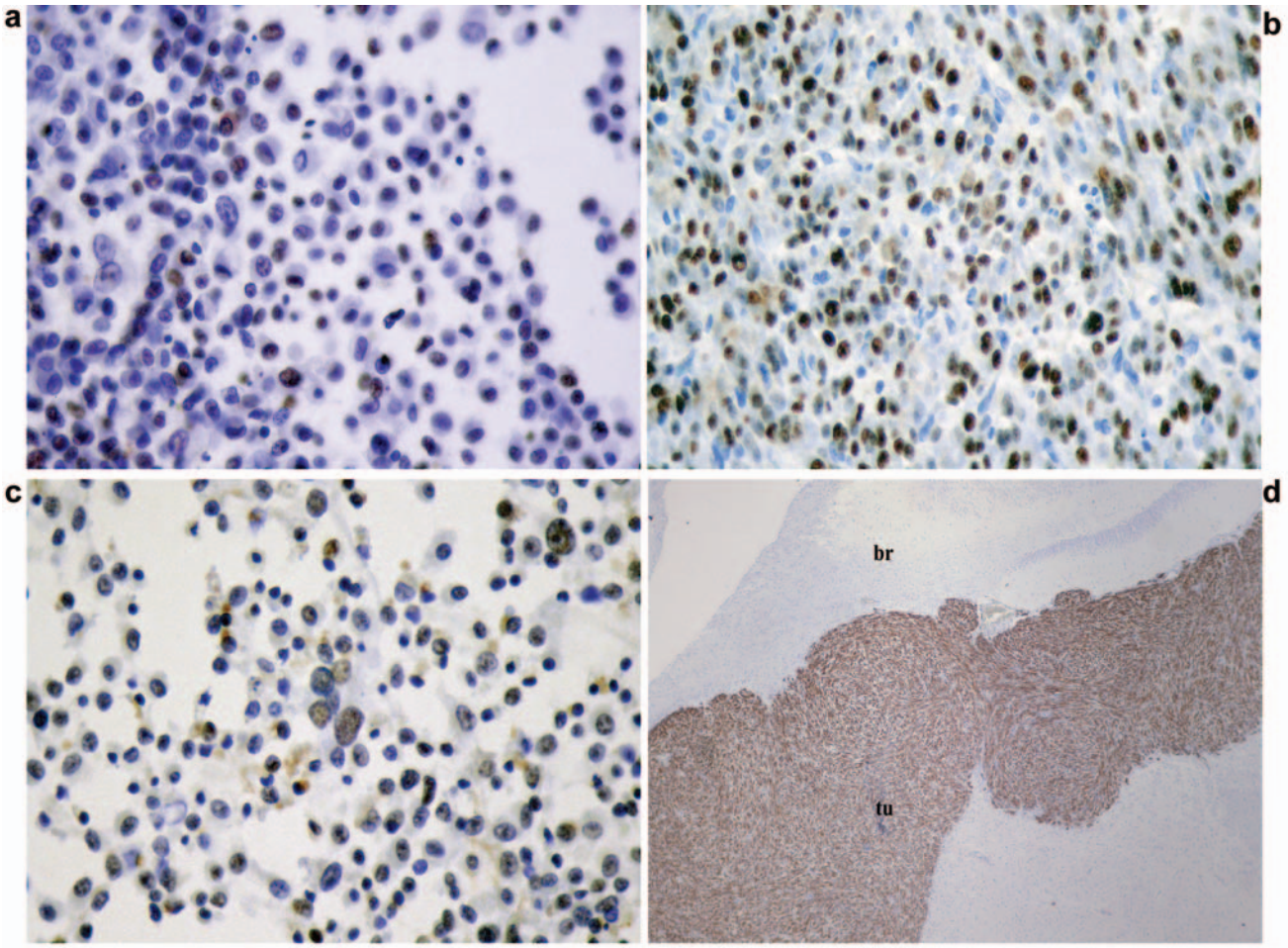

Figure 6. →

Table I. *Immunohistochemistry of U87 cell smears, spheroids and tumour samples.*

Samples	U87 susp.	Sph-I gen.	Sph-II gen.	Sph-III gen.	Tu-I gen.	Tu-II gen.	Tu-III gen.
Markers***	No.=5	No.=3	No.=3	No.=3	No.=5	No.=3	No.=2
Ki-67 LI*	45%	55%	30%	40%	75%	80%	78%
p53**	pos.	0	/	/	0	/	/
Vimentin	+++	+++	+++	+++	+++	+++	+++
S100	++	/	+	+	+	+	+
GFAP	++	0	0	0	0	0	0
Nestin	+	0	0	/	++	++	++
Musashi	+	++	++	/	++	+++	++
Synaptophysin	++	0	+	+	+	+	+
Cathepsin B	+++	+++	++	+	+++	++	+
Cathepsin L	+++	++	++	++	+	++	+
CD68	+++	+++	+++	+++	+++	+++	+++
FVIII	0	0	0	/	+	+++	+++
Kallikrein 6	+++	+++	+++	+++	+++	+++	+++

susp. = cell suspension; Sph-I (II, III) gen = first (second, third) generation spheroids; Tu-I (II, III) gen. = first (second, third) generation tumour; No. = number of samples; GFAP = glial fibrillary acidic protein. *percentage of K-67-positive nuclei (mean value of samples); **pos. = positive (>10% of the tumour cells showed p53 nuclear staining); 0 = negative; / = no data; ***immunoreactivity for other brain-associated cell markers listed in the Table was evaluated as negative (0) when no positive cells were observed within the tumour, weak (+) when <30% of the tumour cells were positive, moderate (++) when 30-60% of the tumour cells were positive and strong (+++) when >60% of tumour cells were positive.

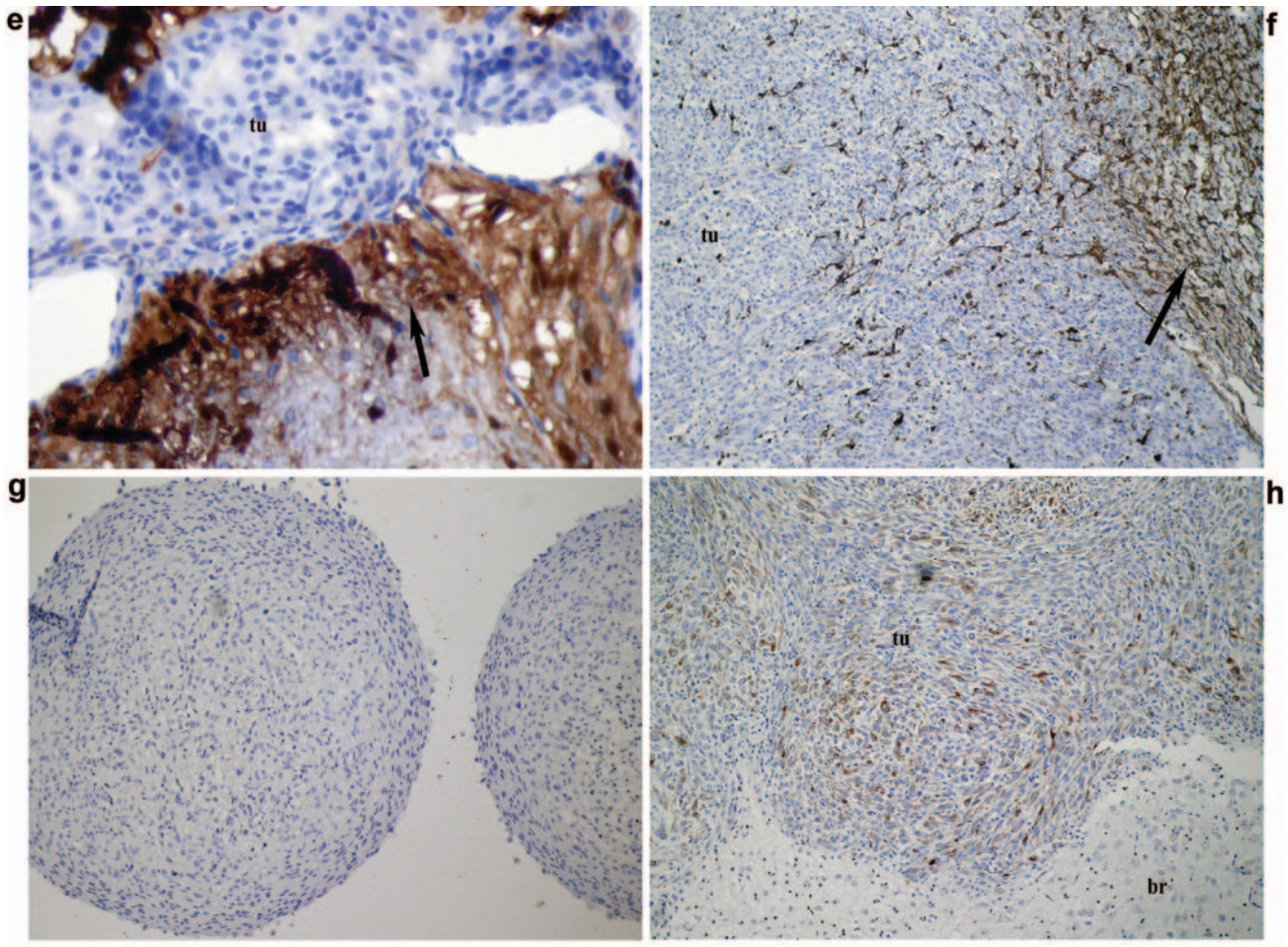

Figure 6. *Immunostaining was evaluated as described in Materials and Methods. a) Numerous Ki-67-positive nuclei in the U87 cell suspension and b) in the tumour (x40). c) Smear preparation of the U87 cell suspension with numerous p53-positive nuclei (x40). d) Most of the tumour cells presented a strong immune reaction for vimentin (x4). e) The expression of S100 protein was minimal in the tumour cells. Strong immunostaining for S100 protein was noted in the surrounding normal and oedematous brain tissue, especially for reactive astrocytes (arrow) (x10). f) Tumours were GFAP-negative, whereas normal and oedematous brain tissue showed an intense expression of GFAP in nearly all the astroglial cells (arrow) (x10). g) Spheroids negative for nestin (x10). h) The expression of nestin was moderately increased in the tumour cells and vascular endothelia (x10).*

reaction, especially at the periphery (Figure 7d). The expression of cathepsin L in the tumour cells of the tumours was weaker, whereas there was no reaction in the vascular endothelia. The cortical pyramidal cells also stained positive for cathepsin L. Staining with the CD68 antibody revealed a strong positive reaction in most of the cells in suspension, spheroids and in tumours of all three generations (Figure 7e,f). The tumour periphery, with widespread leukocyte infiltration, showed only weak immunoreactivity for the CD68 antibody, whereas perivascular cell cuffs near the tumour showed a strong positive reaction. There was no expression of FVIII in the tumour cells in suspension and in the spheroids, whereas tumour and normal brain vascular endothelia displayed a strong positive reaction (Figure 7g). Most of the tumour cells in suspension, spheroids and in tumours of all three generations presented a strong immune reaction for kallikrein 6, whereas the expression in the vascular endothelia of the tumour and in the surrounding brain was weak or absent. Normal and oedematous rat brain tissue showed weak expression of kallikrein (Figure 7h).

Discussion

Xenograft models of experimental and human gliomas have been used for different purposes in recent years (1, 2). The main objective of the present work was to develop a simple and cheap animal model, with high tumour take rate, for brain tumour progression studies. The macroscopic tumour appearance, histopathology and immunohistochemistry of selected relevant tumour progression markers were

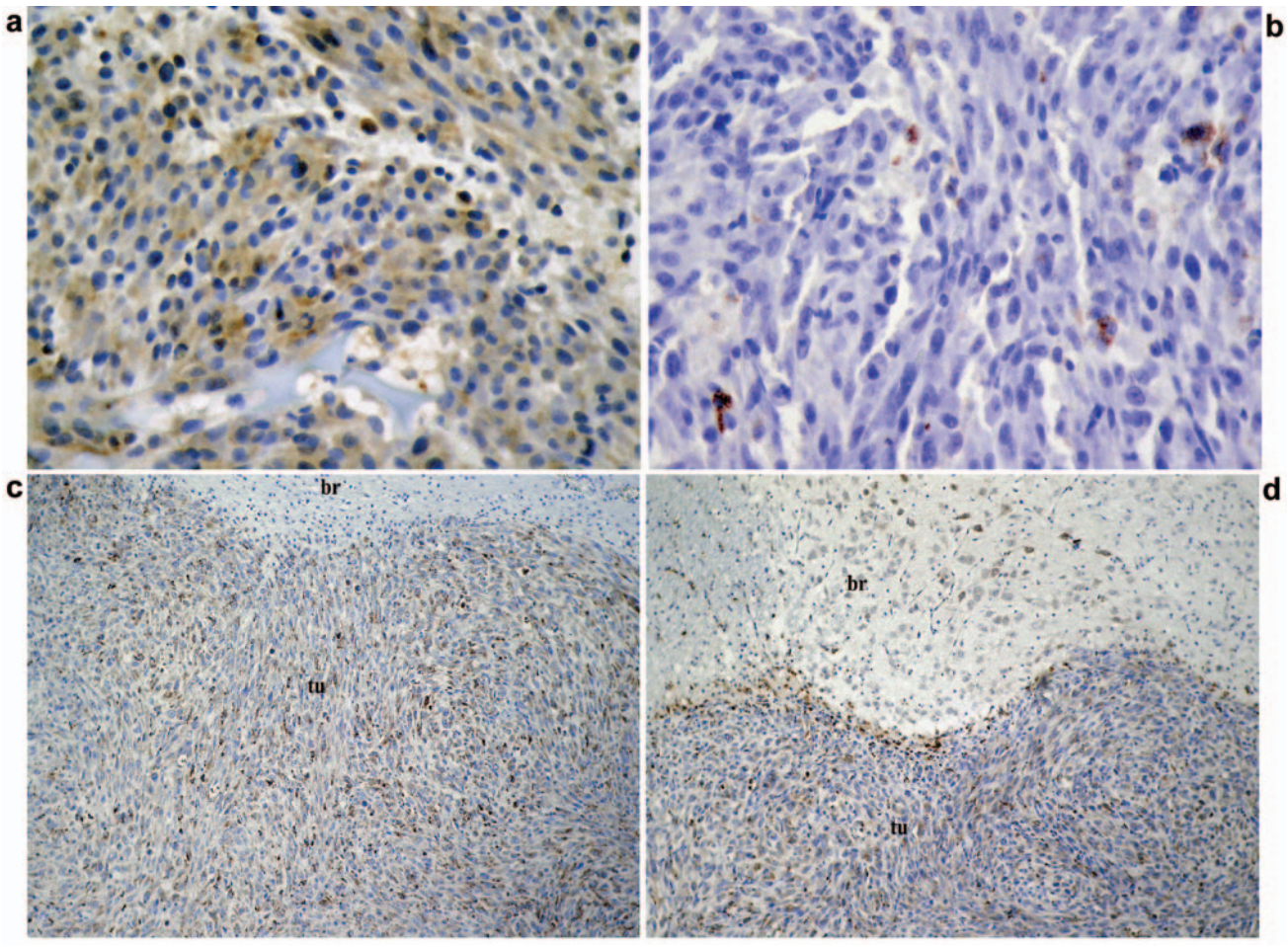

Figure 7. →

monitored in U87 human glioblastoma cells xenografted into the brain of immunosuppressed rats.

In accordance with other reports, maximum progressive tumour growth was observed after 3 weeks (1). However, some authors had not sacrificed the animals before 3 months (7), which may have caused problems due to the host's immune reaction, in spite of the fact that the brain is considered to be an immunologically privileged site (15). In our hands, suppression with cyclosporin A resulted in rapid tumour formation with no signs of transplant rejection, when the animals were sacrificed in the 2 to 3-week period. After the first week, the leukocyte infiltration was pronounced around the tumour, whereas after the second and third weeks this infiltration had diminished, as also described by Wechsler *et al.* (1) and Hossmann *et al.* (16). According to the WHO classification of human brain tumours (17), the transplantation tumours demonstrated features of anaplastic astrocytic tumour (WHO grade III), but became increasingly similar to glioblastomas (WHO grade IV) in the second and third generations. Parallel to this progression, increasing neovascularization and tumour necrosis was observed, both characteristic of glioblastoma.

The benefits of inoculation of pre-cultured small tumour spheroids have been well described (5, 7). However, it should be stressed that spheroids from a biopsy specimen consist of heterogeneous cell populations, *e.g.,* vascular elements (endothelial cells, pericytes), other mesenchyme-derived cells (fibroblasts) and microglia (a type of differentiated tissue macrophage) (4, 18), requiring more careful characterization of the cellular composition of the inoculated spheroids when interpreting the resulting tumour behaviour. In contrast, U87 cell-inoculated tumours have a relatively isomorphous cellular composition, due to their clonal origin, and further tumour development can be followed during subsequent generations, with respect to dedifferentiation of the tumour cells and induced recruitment of stromal cells from the tumour microenvironment (19).

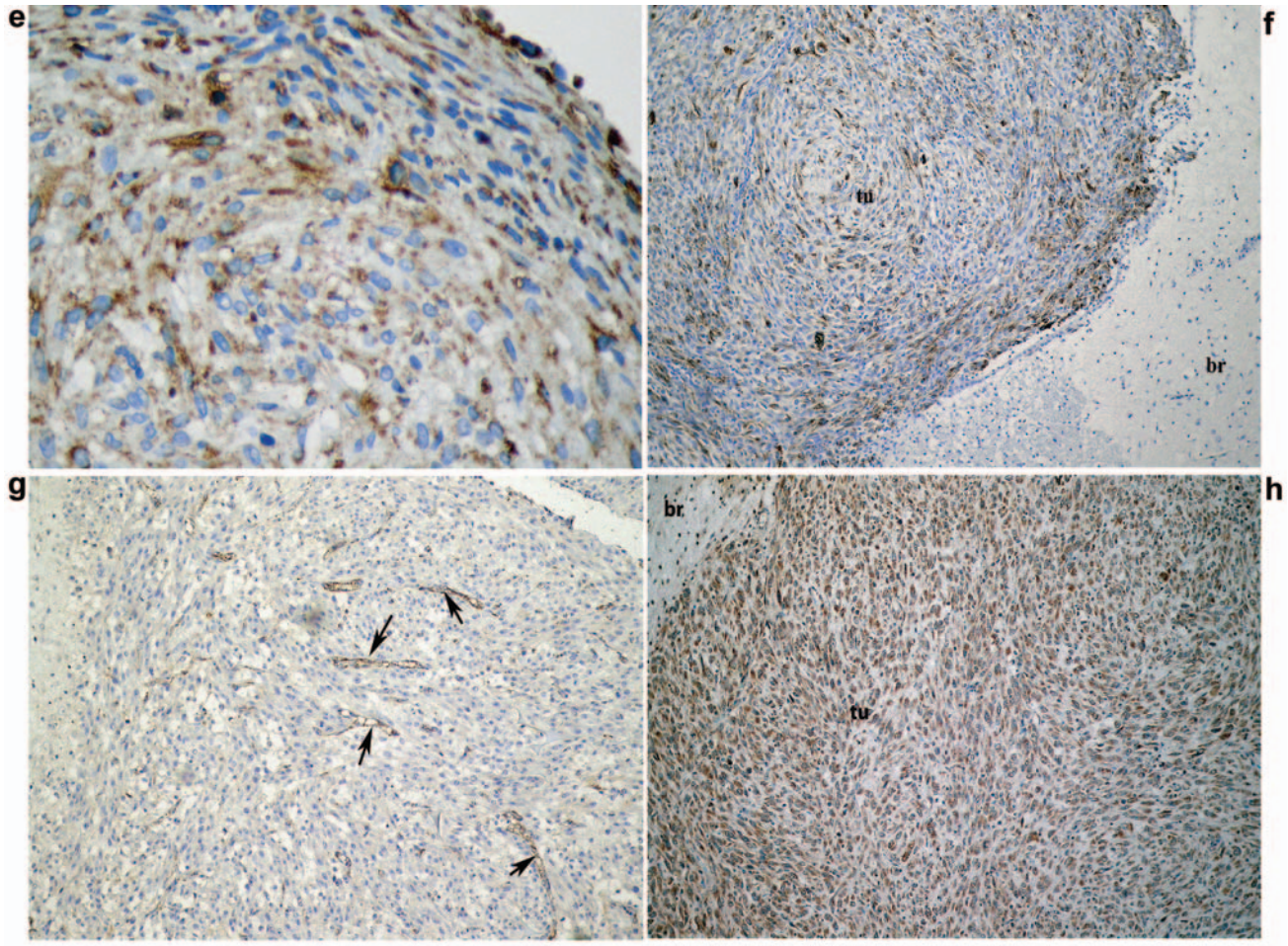

Figure 7. *a) Moderate immunoreactivity for musashi inside the tumour (x40). b) Synaptophysin expression in tumour cells was minimal (x40). c) Diffuse positive immune reaction for cathepsin B inside the tumour (x10). d) The expression of cathepsin L in the tumour cells of the tumours was stronger on the periphery (x10). e) Staining with CD68 antibody revealed a strong positive reaction in most spheroids (x40). f) The same was found in tumours of all three generations (x10). g) Inside the third generation tumour, numerous tumour blood vessels could be observed (arrows) (x10). h) Most of the tumour cells inside the tumours of all three generations presented a strong immune reaction for kallikrein 6 (x10).*

Ki-67 antigen expression is a measure of the proportion of cellular and, hence, biological aggressiveness in malignancy (20, 21). The proliferative activity, defined by the Ki-67 LI, was correlated with progression and prognosis in a number of malignant tumours including prostate cancer (22). We found higher levels of this antigen in the first, second and third generation tumours compared to the U87 cell suspension and the spheroids, indicating increased proliferation in this model of tumorigenicity.

Vimentin is an intermediate filament protein, which marks the mesenchymal cell phenotype. In the course of development of the nervous system, vimentin appears first in immature glial cells (23), but rapidly decreases as GFAP appears concomitantly with myelination (24). In mature astroglia, vimentin and GFAP coexist, and normal, reactive and neoplastic astrocytes have been found to contain variable amounts of both (25). In the present work, it was revealed that high production of vimentin by the tumour cells was preserved in tumour progression in the host, thus showing that the U87 clone consists of immature cells.

S100 and its subunits have been identified in a wide variety of normal, reactive and neoplastic human tissues (26, 27) and determined both in biopsies of glial tumours and their established primary cell cultures (28, 29). Only moderate S100 immunoreactivity was detected in the U87 cell suspension and weak expression in the tumour induced by injection of spheroids or implantation of tumour tissue, which can be explained by the possible down-regulation of S100 expression following tumour dedifferentiation (4).

GFAP represents one of the five essential cytoskeletal components of most vertebrate eukaryotic cells (30) and is restricted to mature astrocytes. The U87 cell suspension presented a moderate immune reaction for GFAP, but it was absent in the induced tumours. This does not necessarily mean that a cell is of non-glial origin, but similarly to that observed for S100, the ability to synthesise GFAP after further dedifferentiation of theU87 cells in the host was gradually lost.

Nestin has been detected in primary central nervous system tumours (31). We showed that nestin could be used as a biological marker for glioma malignancy (32). Contrary to the weak nestin expression of the U87 clone in cell cultures, immunostaining was absent in the spheroids. A switch to further dedifferentiation in the host might explain the moderate staining in the Tumour-I generation induced by inoculation of U87 cells or spheroids, as well as in the Tumour-II and -III generations induced by implantation of tumour tissue.

In mammals, the musashi family controls neural stem cell homeostasis, differentiation and tumorigenesis by repressing translation of particular mRNAs (33). The U87 cell suspension presented a weak immune reaction for musashi and, in contrast to nestin, its expression increased in the tumour cells as the tumours progressed, perhaps related to their malignant growth and dedifferentiation.

Synaptophysin is a useful marker for the identification of normal neuroendocrine cells and neuroendocrine neoplasm (34). The expression of synaptophysin decreased from moderate in the U87 cell suspension to weak in the induced tumours. Further dedifferentiation in the host might explain this loss of expression.

Lysosomal cathepsins (Cats) comprise intracellular proteinases of different classes. The malignant progression of human gliomas was first found to be associated with an increase in cysteine proteases, as described by Levicar *et al.* (35). Demchick *et al.* (36) also described high levels of Cat B in tumour and endothelial cells of tumour tissue. In our previous study, we concluded that specific immunostaining of Cat B in tumours, and particularly in endothelial cells, can be used to predict the risk of death in patients with primary tumours of the central nervous system (37). Strong immunostaining for Cat B in the U87 cell suspension and in the first generation, but not in other generation spheroids, indicated that these highly proliferative tumours had lost some of their invasive potential. A closer relationship to *in vitro* tumour cell invasiveness, but not to the tumorigenic potential of tumour cells, was also observed in our breast cancer cell model (38, 39). In agreement with our previous study, Cat B, but not Cat L, staining was observed in endothelial cells of neovessels in higher tumour generations. Sivaparvathi *et al.* (40) demonstrated that Cat L expression and activity also correlated positively with the increasing malignancy of human glioma. We demonstrated Cat L immunolabelling in glioma tissue sections, where it was mostly localized to the tumour cells and was significantly higher in malignant than in benign gliomas (41). Although Cat L protein expression correlated to that of Cat B, Cat L was localized more selectively to the malignant tumour cells, implying its specific role in the malignant transformation of brain tumour cells. Here, a high expression of Cat L was observed in the U87 cell suspension, which decreased in all tumours induced by injection of spheroids and even more in the tumours induced by implantation of tumour tissue, probably because of tumour cell dedifferentiation.

CD68 is a specific marker for resting microglia (42). Considered as immune effector cells of the central nervous system, the microglia represent a major component of the inflammatory cells found in malignant gliomas (43). The role of microglia in malignant glioma biology remains unclear. On the one hand, the microglia may represent a central nervous system antitumour response, which is inactivated by the local secretion of immunonosuppressive factors by glioma cells. On the other hand, taking into account that the microglia are capable of secreting a variety of immunomodulatory cytokines, it is possible that they are attracted by gliomas to promote tumour growth (18). In accordance with the strong immune reaction for CD68 in all our samples, we believe that microglia accumulation in glial tumours does not merely represent a non-specific reaction to tissue injury, but reflects the participation of these cells in supporting and promoting the invasive phenotype of astrocytoma cells.

Factor VIII-related antigen is synthesized in vascular endothelial cells. Anti-FVIIIrAg antibodies have proved reliable markers for human endothelial cells (44). A strong immune reaction for FVIII was noted in tumours of the second and third generation, which correlated with increased vascular proliferation in more malignant tumours.

Tissue kallikreins also exist as proteases in various tissues including the brain (45-47) and have recently been strongly associated with tumour progression (48). Strong kallikrein 6 immunostaining in the U87 cell suspension and in tumours induced by injection of spheroids and implantation of tumour tissue indicated the role of kallikrein in tumour growth.

Conclusion

In conclusion, the U87 human glioblastoma spheroid cell line model in immunosuppressed Wistar rats provides an excellent system for experimental studies of human malignant brain tumours. The panel of marker protein expressions were followed in the first, second and third generations of tumours. The data indicated that tumour progression was characterised by increased cell proliferation

and tumour cell dedifferentiation, but lower invasiveness of the resulting tumours. However, increased angiogenesis indicated high malignancy of the higher tumour generation. The model provides the basis for further multigenetic and multimolecular tumour cell analyses.

Acknowledgements

This work was supported by the projects Nb L3-6269-0334-04 and Nb P3-327 granted to T. S. by the Ministry of Higher Education, Science and Technology of the Republic of Slovenia. We thank Prof. Dr. Eleftherios P. Diamandis from Mount Sinai Hospital, Toronto, Canada, for providing us with the human kallikrein 6 serine protease polyclonal antibodies. We also thank Prof. Dr. Rolf Bjerkvig, Bergen University, Bergen, Norway, for providing the nestin and musashi polyclonal antibodies.

References

1 Wechsler W, Szymas J, Bilzer T and Hossmann KA: Experimental transplantation gliomas in the adult cat brain. Aca Neurochirurg *98*: 77-89, 1989.

2 Pilkington GJ, Bjerkvig R, De Ridder L and Kaaijk P: *In vitro* and *in vivo* models for the study of brain tumour invasion. Anticancer Res *17*: 4107-4110, 1997.

3 Brem H and Sawaya R: Brain tumours: general considerations. *In*: Youmans Neurological Surgery, 5th ed., Winn HR (ed.). Vol 1. New York, W.B. Saunders, pp. 659-660, 2004.

4 Bressler J, Smith BH and Kornblith PL: Tissue culture techniques in the study of human gliomas. *In*: Neurosurgery. Wilkins RH (ed.). New York, Mc Graw Hill, pp. 542-548, 1985.

5 Bjerkvig R, Tønnesen A, Laerum OD and Backlund EO: Multicellular tumour spheroids from human gliomas maintained in organ culture. J Neurosurg *72*: 463-475, 1990.

6 Engebraaten O, Bjerkvig R, Lund-Johansen M, Wester K, Pedersen P-H, Mørk S, Backlund E-O and Laerum OD: Interaction between human brain tumour biopsies and fetal rat brain tissue *in vitro*. Acta Neuropathol (Berl) *81*: 130-140, 1990.

7 Engebraaten O, Hjortland GO, Hirschberg H and Fodstad O: Growth of precultured human glioma specimens in nude rat brain. J Neurosurg *90*: 125-132, 1999.

8 Fogh J, Wright WC and Loveless JD: One hundred and twenty-seven cultured human tumour cell lines producing tumours in nude mice. J Natl Cancer Inst *59*: 221-226, 1977.

9 Ponten J and Macintyre EH: Long-term culture of normal and neoplastic human glia. Acta Pathol Microbiol Scand *74*: 465-486, 1968.

10 Olopade OI, Jenkins RB, Ransom DT, Malik K, Pomykala H, Nabori T, Cowan JM, Rowler JD and Diaz MO: Molecular analysis of deletions of the short arm of chromosom 9 in human gliomas. Cancer Res *52*: 2523-2529, 1992.

11 Sabattini E, Bisgaard K, Ascani S, Poggi S, Piccioli M, Ceccarelli C, Pieri F, Fraternali-Orcioni G and Pileri SA: The EnVision++system: a new immunohistochemical method for diagnostics and research. Critical comparison with the APAAP, ChemMate, CSA, LABC, and SABC techniques. J Clin Pathol *51*: 506-511, 1998.

12 Li R, Heydon K, Hammond ME, Grignon DJ, Roach M, Wolkov HB, Sandler HM, Shipley WU and Pollack A: Ki-67 staining index predicts distant metastasis and survival in locally advanced prostate cancer treated with radiotherapy. Clin Cancer Res *10*: 4118-4124, 2004.

13 Takeuchi H, Ozawa S, Ando N, Kitagawa Y, Ueda M and Kitajima M: Cell-cycle regulators and the Ki-67 labeling index can predict the response to chemoradiotherapy and the survival of patients with locally advanced squamous cell carcinoma of the esophagus. Ann Surg Oncol *10*: 792-800, 2003.

14 Almqvist PM, Mah R, Lendahl U, Jacobsson B and Hendson G: Immunohistochemical detection of nestin in pediatric brain tumours. J Histochem Cytochem *50*: 147-158, 2002.

15 Dietrich P-Y, Walker PR and De Tribolet N: Aspects of immunology applicable to brain tumour pathogenesis and treatment. *In*: Youmans Neurological Surgery. Winn HR (ed.). 5th ed., Vol 1. New York, W.B. Saunders, pp. 887-897, 2004.

16 Hossmann K-A, Wechsler W and Wilmes F: Experimental peritumourous edema. Morphological and pathophysiological observations. Acta Nuropathol *45*: 195-203, 1979.

17 Kleihues P and Cavenee WK: Pathology and genetics of tumours of the nervous system. WHO Classification of Tumours. Lyon: IARC Press, pp. 9-54, 2000.

18 Badie B and Schartner J: Role of microglia in glioma biology. Microscop Res Techn *54*: 106-113, 2001.

19 Mueller MM and Fusenig NE: Friends or foes – bipolar effects of the tumour stroma in cancer. Nat Rev Cancer *4*: 839-849, 2004.

20 Scott R, Hall P and Haldane J: A comparison of immuno-histochemical markers of cell proliferation with experimentally determined growth fraction. J Clin Pathol *165*: 173-178, 1991.

21 Wilson G, Saunders M and Dische S: Direct comparison of bromodeoxyuridine and Ki-67 labeling indices in human tumours. Cell Prolif *29*: 141-152, 1996.

22 Halvorsen OJ, Haukaas S, Hoisaeter PA and Akslen LA: Maximum Ki-67 staining in prostate cancer provides independent prognostic information after radical prostatectomy. Anticancer Res *21*: 4071-4076, 2001.

23 Dahl D, Rueger DC and Bignami A: Vimentin, the 57,000 molecular weight protein of fibroblast filaments, is the major cytoskeletal component in immature glia. Eur J Cell Biol *90*: 191-196, 1981.

24 Dahl D: The vimentin-GFAP protein transition in rat neuroglia cytoskeleton occurs at the time of myelination. J Neurosci Res *6*: 741-748, 1981.

25 Yung WKA, Luna M and Borit A: Vimentin and glial fibrillary acidic protein in human brain tumours. J Neurooncol *3*: 35-38, 1985.

26 Takahashi K, Isobe T and Ohtsuki Y: Immunohistochemical study of the distribution of and subunits of S100 protein in human neoplasm and normal tissues. Virchows Arch B *45*: 385-396, 1984.

27 Kahn HJ, Marks A and Thom H: Role of antibody of S100 protein in diagnostic pathology. Am J Clin Pathol *79*: 341-347, 1983.

28 Bigner DD, Bigner SH, Ponten J, Westermark B, Mahaley MS Jr, Rouslahti E, Herschman H, Eng LF and Wikstrand CJ: Heterogeneity of genotypic and phenotypic characteristics of fifteen permanent cell lines derived from human gliomas. J Neuropathol Exp Neurol *40*: 201-229, 1981.

29 Jacque CM, Kujas M, Poreau A, Raoul M, Collier P, Racadot J and Baumann N: GFA and S100 protein levels as an index for malignancy in human gliomas and neurinomas. JNCI *62*: 479-483, 1979.

30 Lazarides E: Intermediate filaments: a chemically heterogeneous, developmentally regulated class of proteins. Annu Rev Biochem *51*: 219-250, 1982.

31 Dahlstrand J, Collins VP and Lendahl U: Expression of the Class VI intermediate filament nestin in human central nervous system tumours. Cancer Res *52*: 5334-5341, 1992.

32 Strojnik T: Immunohistochemical detection of nestin and musashi in tumour and endothelial cells and their role as possible prognostic factor for survival in glioma patients. Anticancer Res *24(5D)*: 3642, 2004. (Abstracts of the Seventh International Conference of Anticancer Research, Corfu, Greece, October 25-30, 2004.

33 Okano H, Imai T and Okabe M: Musashi: a translational regulator of cell fate. J Cell Science *115*: 1355-1359, 2002.

34 McKeever PE: Insights about brain tumours gained through immunohistochemistry and *in situ* hybridization of nuclear and phenotypic markers. J Histochem Cytochem *46*: 585-594, 1998.

35 Levicar N, Nuttall RK and Lah TT: Proteases in brain tumour progression. Acta Neurochir (Wien) *145*: 825-838, 2003.

36 Demchik LL, Sameni M, Nelson K, Mikkelsen T and Sloane BF: Cathepsin B and glioma invasion. Int J Dev Neurosci *17(5-6)*: 483-494, 1999.

37 Strojnik T, Kos J, Zidanik B, Golouh R and Lah T: Cathepsin B immunohistochemical staining in tumour and endothelial cells is a new prognostic factor for survival in patients with brain tumours. Clin Cancer Res *5*: 559-567, 1999.

38 Zajc I, Sever N, Bervar A and Lah T: Expression of cysteine peptidase cathepsin L and its inhibitors stefins A and B in relation to tumorigenicity of breast cancer cell lines. Cancer Lett *187*: 185-190, 2002.

39 Bervar A, Zajc I, Sever N, Katunuma N, Sloane BF and Lah TT: Invasiveness of transformed human breast epithelial cell lines is related to cathepsin B and inhibited by cysteine proteinase inhibitors. Biol Chem *384*: 447-455, 2003.

40 Sivaparvathi M, Sawaya R, Wang SW, Rayford A, Yamamoto M, Liotta LA, Nicolson G and Rao JS: Overexpression and locallization of Cat B during the progression of human gliomas. Clin Exp Metastasis *13*: 49-56, 1995.

41 Strojnik T, Kavalar R, Trinkaus M and Lah T: Cathepsin L in glioma progression: comparison with cathepsin B. Cancer Det Prev *29*: 448-455, 2005.

42 Hulette CM, Downev BT and Burger PC: Macrophage markers in diagnostic neuropathology. Am J Surg Pathol *16*: 493-499, 1992.

43 Badie B, Schartner JBS, Klaver J and Vorpahl J: *In vitro* modulation of microglia motility by glioma cells is mediated by hepatocyte growth factor/scatter fator. Neurosurg *44*: 1077-1082, 1999.

44 McComb RD, Jones TR and Pizzo SV: Specificity and sensitivity of immunohistochemical detection of factor VIII/von Willebrand factor antigen in formalin-fixed paraffin-embedded tissue. J Histochem Cytochem *30*: 371-377, 1982.

45 Borgono CA and Diamandis EP: The emerging roles of human tissue kallikreins in cancer. Nature Rev Cancer *4*: 876-890, 2004.

46 Borgono CA, Michael IP and Diamandis EP: Human tissue kallikreins: physiologic roles and applications in cancer. Mol Cancer Res *2*: 257-280, 2004.

47 Raidoo DM, Snyman C, Narotam PK, Muller R and Bhoola KD: Human cerebral tissue kallikrein. Asia Pac J Pharmacol *10 (Suppl 1)*: S72, 1995.

48 Diamandis EP, Yousef GM and Olsson AY: An update on human and mouse glandular kallikreins. Clin Biochem *37*: 258-260, 2004.

Received February 27, 2006
Revised April 28, 2006
Accepted May 15, 2006